

AC Loss Modeling in $\text{Ba}_{0.5}\text{Sr}_{0.5}\text{TiO}_3$ Using Dielectric Relaxation

Nadia K. Pervez¹, Jiwei Lu², Susanne Stemmer², Robert A. York¹

¹Department of Electrical and Computer Engineering, University of California, Santa Barbara, CA 93106, U.S.A.

²Materials Department, University of California, Santa Barbara, CA 93106, U.S.A.

ABSTRACT

In universal relaxation, a material's complex dielectric susceptibility follows a fractional power law f^{1-n} where $0 < n < 1$ over multiple decades of frequency. In a variety of materials, including $\text{Ba}_{0.5}\text{Sr}_{0.5}\text{TiO}_3$, dielectric relaxation has been observed to follow this universal relaxation model with values of n close to 1. In this work we have shown that the universal relaxation model can be used to calculate dielectric loss even when n is very close to 1. Our calculated Q-factors agree with measured values at 1 MHz; this agreement suggests that this technique may be for higher frequencies where network analyzer measurements and electrode parasitics complicate Q-factor determination.

INTRODUCTION

Universal relaxation refers to behavior where a material's complex dielectric susceptibility is observed to follow a decreasing power law over multiple decades in frequency [1]. This behavior is observed in a variety of different materials including $\text{Ba}_x\text{Sr}_{1-x}\text{TiO}_3$, Al_2O_3 , Ta_2O_5 , HfO_2 , and SiO_2 [2,3]. It appears to be a property of extrinsic disorder rather than an intrinsic material property [4,5]. The susceptibility shows an f^{1-n} frequency dependence, where $0 < n < 1$. For a lossless material, $n=1$. A direct consequence of this power law is that if the real component of a material's complex susceptibility obeys a power law, so must the imaginary component.

While many materials have been observed to obey Curie-von Schweidler behavior, corresponding to $n \sim 1$, little attention has been focused on the corresponding loss predictions using the universal relaxation model. Even when little relaxation is observed – when n is very close to 1 – the model can still accurately predict loss. The ability to calculate losses from capacitance data may be advantageous in situations where the direct measurement of Q-factors is difficult, such as network analyzer measurements of low-loss films. Reflection-type measurements of high-Q reactive loads performed with network analyzers are less accurate than auto-balancing bridge measurements performed with impedance analyzers. However, auto-balancing bridge measurements are limited to below 110 MHz. Provided that parasitic electrode inductances at high frequencies can be accounted for, this technique offers an accurate way to indirectly measure film loss through capacitance measurements.

In $\text{Ba}_{0.5}\text{Sr}_{0.5}\text{TiO}_3$ (BST) we have successfully used power-law capacitance data to predict Q-factor values. Comparison of 1 MHz Q-factors calculated and measured using an impedance analyzer demonstrates the validity of this approach. The calculated values are consistently equal to or slightly higher than measured values, consistent with the expected small contribution of series electrode resistance to measured Q-factors at 1MHz. Based on the successful application

of this technique at low frequencies, we performed high frequency measurements on BST thin film capacitors, using the observed dielectric relaxation to calculate the films' Q-factors.

EXPERIMENTAL DETAILS

Capacitance and Q measurements were performed on parallel plate capacitors with a coplanar probe G-S-G configuration. The $\text{Ba}_{0.5}\text{Sr}_{0.5}\text{TiO}_3$ (BST) films used for these measurements were deposited by RF-magnetron sputtering on to platinumized c-plane sapphire substrates. A mesa isolation etch was performed in buffered HF, and top electrodes were formed using electron-beam evaporation and lift-off of Pt. In order to minimize probe pad parasitics, the coplanar probes were landed directly on the devices, constraining the minimum device area to the size of the probe footprint, $12\ \mu\text{m} \times 12\ \mu\text{m}$. The maximum device area was $45\ \mu\text{m} \times 45\ \mu\text{m}$.

Capacitance and Q measurements were performed using an Agilent 4294A impedance analyzer for measurements from 40 Hz to 110 MHz. An Agilent 8722D network analyzer was used for measurements from 50 MHz to 40 GHz, and an Agilent E8362B PNA series network analyzer was used for capacitance measurements from 10 MHz to 20 GHz. For high frequency measurements, where the parasitic electrode inductance resulted in an L-C resonance, the measured resonance frequency and low frequency capacitance were used to calculate an approximate electrode inductance. The contribution of this parasitic inductance was subtracted from the measured reactance to determine the device capacitance.

DISCUSSION

Fractional power law

Universal relaxation refers to a fractional power law behavior in the real and imaginary parts of the dielectric susceptibility. These quantities are related by the Kramers-Kronig relations. Thus when we find a fractional power law in the real part of the susceptibility – and therefore the capacitance – we also know the form of the dielectric loss associated with that capacitance. More specifically, if we observe a capacitance of the form of equation 1 for multiple decades, the loss tangent (inverse Q) must have the form of equation 2.

$$C = C_{\infty} + C_0 \left(\frac{f}{f_0} \right)^{1-n} \quad \text{where } 0 < n < 1 \quad (1)$$

$$Q = \left(\frac{C(f)}{C(f) - C_{\infty}} \right) \tan \left(\frac{n\pi}{2} \right) \quad (2)$$

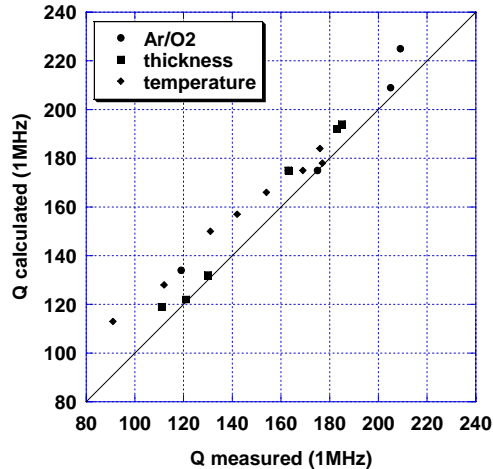


Figure 1. Comparison of measured and calculated Q values at 1 MHz for 3 different measurement series (Ar/O2, thickness, and temperature).

While this is not an intrinsic loss mechanism for BST thin films, it has been observed to be the dominant loss behavior up to 20 GHz [2]. We choose to take advantage of the simple form of the relationship between the measured capacitance and loss associated with it through the transform pair.

Low frequency measurements

Low frequency measurements were performed on a BST sample at different temperatures (temperature series), BST samples grown under different conditions (Ar/O2 series), and BST samples with different film thicknesses (thickness series). Figure 1 compares the measured Q values at 1 MHz with the calculated Q values. The calculated values are in agreement with the measured values. Most of the calculated values at 1 MHz are slightly higher than the measured values. A likely explanation for this is the small contribution of series electrode resistance at this frequency.

Reflection measurements

Network analyzers employ transmission and reflection measurements rather than using auto-balancing bridges like impedance analyzers. A typical 1-port network analyzer calibration uses measurements of an open standard, a short standard, and a 50 ohm load standard. Unfortunately, an acceptable 1-port calibration for loads close to 50 ohms may be terribly inaccurate for capacitor measurements. For non-50 ohm loads, such as our BST capacitors, Q measurement accuracy is low because the measured reflection is close to 1. Figure 2 shows the same capacitance and Q versus voltage measurement performed on both a network analyzer and an impedance analyzer. Note that while the capacitance curves are identical, the Q curves are not. At higher voltages the network analyzer measurement is off by 2 orders of magnitude, and in fact the Q values become negative as the small measured resistance becomes a small negative resistance.

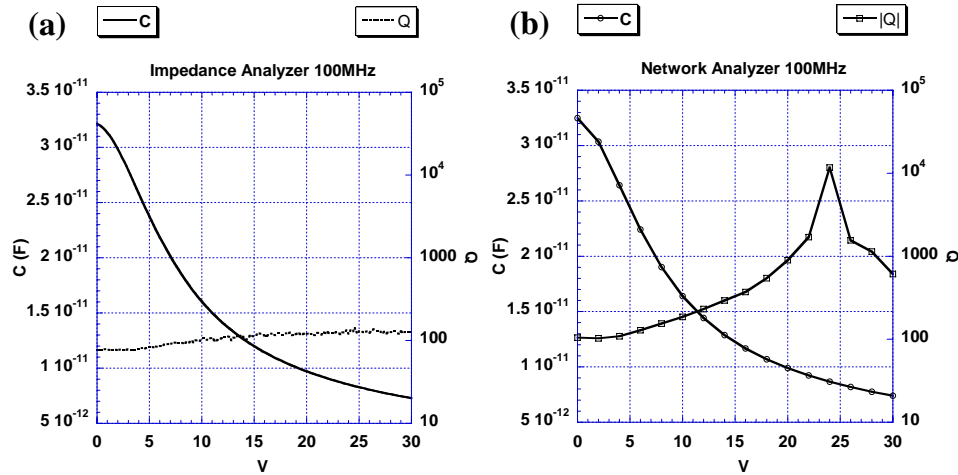


Figure 2. Comparison of (a) network analyzer and (b) impedance analyzer C-V and Q-V measurements at 100 MHz.

The advantage of loss calculations from the capacitance data is clear in figure 2; it is much less arduous to calibrate a network analyzer for a good capacitance measurement than for both good capacitance and Q measurements. Figure 3 shows both the low frequency and high frequency Q values for devices of the same geometry from the same sample. While the uncertainty in the high frequency calculation is much higher than in the low frequency calculation, it is still relatively small.

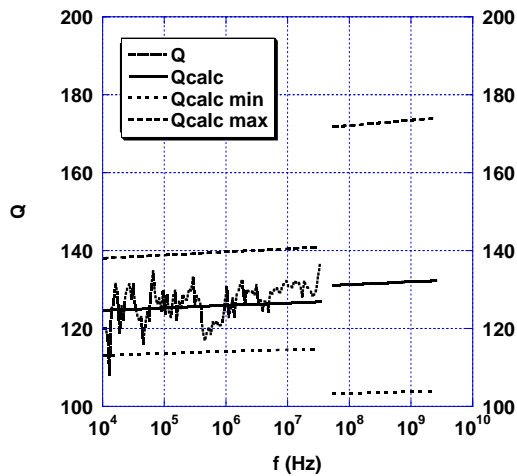


Figure 3. Low frequency measured Q plotted together with low and high frequency calculated Q values.

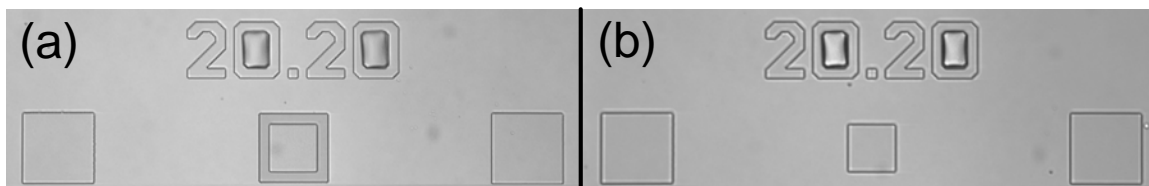


Figure 4. Picture of (a) normal device and (b) “shorted” structure.

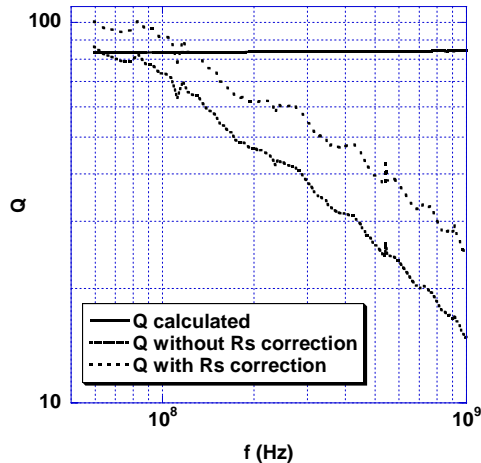


Figure 5. Comparison of calculated Q value with measured Q values with and without series resistance correction (R_s).

Loss contributions

At GHz frequencies series electrode losses result in a dramatic decrease in measured Q values. Part of this series electrode resistance can be accounted for through the measurement of a “shorted” structure, such as the one shown in figure 4, where the BST has been completely etched away before top electrode deposition. While this does lead to a small correction in Q, it fails to capture the frequency dependent series resistance contribution from the electrode-film interfaces. Figure 5 shows data with and without the measured series resistance contribution, along with the Q calculated from the capacitance data. One of the advantages of the calculation is that only resistances in parallel to the capacitance contribute to the calculated Q. This is highly advantageous at high frequencies (such as in figure 5) where series electrode contributions dominate measured Q values.

CONCLUSIONS

We have successfully shown that using the universal relaxation model, we can calculate Q values that agree well with our impedance analyzer measurements. We have also shown that the model can be used to calculate Q values at higher frequencies where measurement capabilities are limited. The high frequency calculation values show the same trend measured at lower frequencies. A direct benefit of this technique is its insensitivity to series electrode resistance, which is otherwise difficult to de-embed.

ACKNOWLEDGEMENTS

This work was supported by DARPA and DMEA through the Center for Nanoscience Innovation for Defense program (CNID) under award number DMEA90-02-2-0215, and by the ARO through the Multifunctional Adaptive Radio Radar and Sensors program (MARRS MURI)

under award number DAAD19-01-1-0496, and by the ONR through the Center for Advanced Nitride Electronics program (CANE MURI) under award number N0014-01-1-0764.

REFERENCES

1. A.K. Jonscher, *J. Phys.D: Appl. Phys.*, **32**, R57-R70 (1999).
2. J.D. Baniecki, R.B. Laibowitz, T.M. Shaw, P.R. Duncombe, D.A. Neumayer, D.E. Kotecki, H. Shen, and Q.Y. Ma, *Appl. Phys. Lett.*, **72**, 498-500 (1998).
3. H. Reisinger, G. Steinlesberger, S. Jakshik, M. Gutsche, T. Hecht, M. Leonhard, U. Schroder, H. Seidl, and D. Schumann, *IEDM Tech. Digest*, 12.2.1-4 (2001).
4. D.P. Almond, and C.R. Brown, *Phys. Rev. Lett.* **92**, 157601-1 (2004).
5. J.R. Jameson, W. Harrison, P.B. Griffin, and J.D. Plummer, *Appl. Phys. Lett.* **84**, 3489 (2004).